Research Article

Journal of Applied Toxicology

Received: 8 September 2014, Revised: 13 November 2014, Accepted: 28 November 2014 Published online in Wiley Online Library

(wileyonlinelibrary.com) DOI 10.1002/jat.3109

Quantitative evaluation of the pulmonary microdistribution of TiO_2 nanoparticles using X-ray fluorescence microscopy after intratracheal administration with a microsprayer in rats

Guihua Zhang[a], Naohide Shinohara[a]*, Hirokazu Kano[b], Hideki Senoh[b], Masaaki Suzuki[b], Takeshi Sasaki[a], Shoji Fukushima[b] and Masashi Gamo[a]

ABSTRACT: The unevenness of pulmonary nanoparticle (NP) distribution, which hinders the establishment of an absolute dose–response relationship, has been described as one of the limitations of intratracheal administration techniques for toxicological assessment of inhaled NPs. Quantification of the NP microdistribution would facilitate the establishment of a concentration–response relationship in localized regions of the lung; however, such quantitative methods have not been reported. Here, we established a quantitative method for evaluating pulmonary TiO_2 NP microdistribution in rats using X-ray fluorescence microscopy. Ti intensity in lung sections from rats intratracheally administered 10 mg kg^{-1} TiO_2 NPs with a microsprayer was measured using X-ray fluorescence with a 100 μm beam size. Ti reference samples were prepared by dropping different concentrations of Ti solutions on glass slide or lung sections of untreated rat. Ti intensity increased linearly with Ti content in the reference samples on both substrates. The detection limit of TiO_2 was estimated to be 6.3 ng mm^{-2}. The reproducibility was confirmed for measurements done in the short- (2 weeks) and long-term (6 months). The quantitative results of TiO_2 NP microdistribution suggested that more TiO_2 NPs were distributed in the right caudal and accessory lobes, which are located downstream of the administration direction of the NP suspension, and the lower portion of each lobe. The detection rates of TiO_2 NPs were 16.6–25.0%, 5.19–15.6%, 28.6–39.2%, 21.4–38.7% and 10.6–23.2% for lung sections from the right cranial, middle, caudal, accessory and left lobes, respectively. Copyright © 2015 John Wiley & Sons, Ltd.

Keywords: intratracheal administration; pulmonary distribution; TiO_2; Ti reference; XRF; rat

Introduction

Titanium dioxide nanoparticles (TiO_2 NPs) have been widely applied in the fields of biomedicine (Yin *et al*., 2013), cosmetics (Su *et al*., 2014) and environmental engineering (Khodadoust *et al*., 2012). However, with the increase in use of TiO_2 NPs, there have been growing concerns about the safety of nanomaterials, including TiO_2 NPs (Shi *et al*., 2013). Indeed, NPs have the greatest potential to deposit in the alveolar region through inhalation exposure.

The intratracheal administration test has been often carried out for the toxicological assessment of inhaled NPs (Jacobsen *et al*., 2009; Sun *et al*., 2012). The unevenness of the pulmonary distribution of NPs, which makes it difficult to establish an absolute dose–response relationship, has been described as one of the limitations of intratracheal administration techniques for the toxicological assessment of inhaled NPs (Brain *et al*., 1976; Driscoll *et al*., 2000; Leong *et al*., 1998). Quantification of the NP microdistribution would facilitate the establishment of a relationship between the content of localized NPs and the pathological responses caused by the administration of NPs in localized regions of the lung. The concentration–response relationship in localized regions is important for our toxicological understanding of NPs when using intratracheal administration techniques. However, quantitative evaluation of the pulmonary microdistribution of NPs has not been performed.

With respect to analytical techniques for measuring NPs in biological tissues, inductively coupled plasma mass spectrometry, inductively coupled plasma atomic emission spectrometry and atomic absorption spectrometry are generally used to determine the concentrations of NPs at the organ–tissue level in experimental animals administered NPs after degradation of the tissues using wet digestion or dry ashing methods (Reuzel *et al*., 1991; Shinohara *et al*., 2014; Sung *et al*., 2009). However, these techniques are not suitable for evaluating the microdistribution of NPs administered in biological tissues. Moreover, radiolabeling techniques have also been used to assess the distribution of fine

*Correspondence to: Naohide Shinohara, National Institute of Advanced Industrial Science and Technology (AIST), Tsukuba, Ibaraki, Japan. Email: n-shinohara@aist.go.jp

[a]National Institute of Advanced Industrial Science and Technology (AIST), Tsukuba, Ibaraki, Japan

[b]Japan Bioassay Research Center, Hadano, Kanagawa, Japan

particles in biological samples (Brain *et al*., 1976; Zhu *et al*., 2009). However, the pretreatment steps required for radiolabeling may change the characterization of particles, affecting the toxicological characteristics of the particles compared with unlabeled particles. In contrast, X-ray fluorescence (XRF) analysis has been considered a useful technique for evaluating the microdistribution of NPs. The main features of XRF are: (i) it is a nondestructive technique; (ii) simultaneous measurement of multiple elements can be performed at all element range from Na to U; and (iii) pretreatment is generally unnecessary.

Regarding the distribution of Ti in biological tissues, Wang *et al*. evaluated the microdistribution of Ti in the olfactory bulb (Wang *et al*., 2007) and the brain (Wang *et al*., 2008) of mice that were intranasally administered with TiO_2 NPs using synchrotron radiation-induced XRF analysis. From their work, distribution maps of the Ti intensities (counts per second, cps), not those of TiO_2 content, were obtained. Therefore, Ti reference samples are necessary for the quantification of TiO_2 content.

Various reference samples have been developed to evaluate quantitatively the distributions of metal elements other than Ti in biological samples using XRF. These samples have been used for clarifying the roles of trace metal elements in the disease process (Auriat *et al*., 2012; Wang *et al*., 2010; Watanabe *et al*., 2001) and for determining the distribution of metal elements in the tissues of rats exposed to the heavy metals (Homma-Takeda *et al*., 2009; Rubio *et al*., 2008). However, accurate quantification is difficult because of different matrices and/or thicknesses between the reference and analytical samples. For example, metal elements (e.g. Ca, Fe, Zn) in brain sections were quantified using pig and bovine liver tablet references (NIST reference material) (Wang *et al*., 2010) or MICROMATTER thin film standards (Auriat *et al*., 2012). Watanabe *et al*. (2001) reported the quantitative mapping of Cu, Fe and Al elements in the sections of liver tissues in primary biliary cirrhosis using reference samples prepared by dropping the metal–organic solutions on a carbon block. Reference samples prepared by embedding metal solutions in polyvinyl alcohol (Homma-Takeda *et al*., 2009) or cellulose and wax (Rubio *et al*., 2008) have been used to quantify the distribution of metal elements (e.g. U, As, Zn, Fe and K) in the kidneys or brains of rats exposed to the heavy metals (e.g. U and As).

No previous studies have provided a quantitative evaluation of the pulmonary microdistribution of Ti or the effects of the matrix in biological samples. Therefore, the aims of the present study were to establish a quantitative method to analyze the pulmonary microdistribution of Ti using XRF microscopy and to evaluate quantitatively the pulmonary microdistribution of TiO_2 NPs in rats intratracheally administered with TiO_2 NPs. To this end, we developed Ti reference samples and created a calibration curve for Ti analysis. Additionally, we investigated the effects of the matrix (lung tissue) and data reproducibility. This study provided insights into the quantitative distribution of TiO_2 NPs following intratracheal administration in rats.

Materials and Methods

Preparation of TiO_2 Suspension

In the present study, AEROSIL® P25 (Nippon Aerosil Co., Ltd, Tokyo, Japan) was used to prepare the suspension of TiO_2 NPs. AEROSIL® P25 has a spherical primary particle size of 21 nm, with a mixture of anatase and rutile phases in a ratio of 80:20. For preparation of the suspension, TiO_2 NPs were added in disodium phosphate solution (2 mg ml^{-1}) and sonicated for 3 h in an ultrasonic bath (5510 J-MT; Branson Ultrasonics Co., USA). The sample was then centrifuged at 1000 *g* for 20 min at 20 °C (CF16RXII; Hitachi Koki Co., Ltd, Japan). The supernatant was collected for the stock suspension. The concentration of the suspension was measured to be 10.3 mg ml^{-1} using a weight scale after drying the suspension in a thermostatic chamber (ON-300S; AS ONE Co., Japan). The *Z*-average diameter of the AEROSIL® P25 suspension, as determined by dynamic light scattering (Zetasizer nano-ZS; Malvern Instruments Ltd., UK), was 132 nm (Fig. 1).

Animals and Husbandry

Male F344/DuCrlCrlj rats (SPF) were obtained at the age of 11 weeks from Charles River Laboratories Japan, Inc. (Kanagawa, Japan). The animals were quarantined and acclimated for 8 days. All animals were housed individually in stainless steel wire hanging cages (170 mm W × 294 mm D × 176 mm H) under controlled environmental conditions (temperature of 23 ± 2 °C and relative humidity of 55 ± 15% with 15–17 air changes per hour) in barrier-controlled animal rooms. Fluorescent lighting was controlled automatically to provide a 12 h light/dark cycle. All rats had free access to sterilized water and γ-irradiation-sterilized commercial basal diet (CRF-1; Oriental Yeast Co., Ltd., Tokyo, Japan). The animals were cared for in accordance with the guidelines for the care and use of laboratory animals (NRC, 1996), and the protocol of the experiment was approved by the Institutional Animal Care and Use Committee at the Japan Bioassay Research Center (JBRC).

Intratracheal Administration and Preparation of Lung Sections

In the present study, the dose of TiO_2 NPs was set relatively high (10 mg kg^{-1}) to evaluate quantitatively the differences in the NP microdistribution among different lung lobes in rats. For evaluation of the pulmonary microdistribution of TiO_2 NPs, 12-week-old male rats were used. After inhalational anesthesia with 2.5% isoflurane gas (Forane; Abbott Japan Co., Ltd., Tokyo, Japan), the rats (weighing 245–250 g) were intratracheally

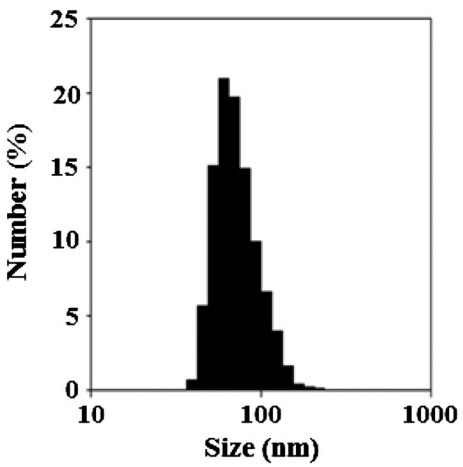

Figure 1. The number-based size distribution of TiO_2 nanoparticle (AEROSIL® P25) suspension (10.3 mg ml^{-1}), as measured by dynamic light scattering. The *Z*-average diameter of AEROSIL® P25 suspension was 132 nm.

Journal of Applied Toxicology

administered a TiO_2 NP suspension (1 ml kg^{-1} BW) at a single dose of 10 mg kg^{-1} body weight (BW; TiO_2-treated rats) using a MicroSprayer Aerosolizer (Model: IA-1B; Penn-Century Inc., Wyndmoor, PA, USA). During intratracheal administration, each rat was supported by a nylon band under its upper incisors and placed on a slanted board (60° from the horizontal direction). The MicroSprayer was inserted 25 mm from the larynx (near the tracheal bifurcation) of the rat.

Rats were euthanized by exsanguination from the abdominal aorta under intraperitoneal pentobarbital anesthesia the day after administration, and the left and right cranial, middle, caudal and accessory lobes of the lungs were separately removed. The lung lobes were then fixed in 10% neutral buffered formalin solution after the tracheas were tied off, and tissue samples were embedded in paraffin. Paraffin-embedded lung tissues were cut into 3 μm thick sections, and the sections were mounted onto glass slides without glass covers and stained with hematoxylin and eosin. Untreated rat was also killed, and lung sections of the left and right lobes were prepared under the same conditions as described above.

X-ray Fluorescence Microscopy and Analytical Conditions

The intensities of Ti in the samples were measured with a high-performance energy-dispersive XRF spectrometer with a rhodium target X-ray tube (XGT-7200; Horiba Int., Kyoto, Japan). The spectral intensity of the Ti-Kα line (4.511 keV; Fig. 2) was acquired for the quantification of Ti in the selected rectangular areas of the samples. The analytical conditions of Ti were set as follows: beam size (spatial resolution), 100 μm; step size, 100 μm and 200 μm for reference samples and lung sections from untreated and TiO_2-treated rats; acquisition time, 60 s $point^{-1}$; excited voltage, 50 kV; excited current, 1 mA; and full vacuum mode. The intensity of Ti in a mesh (100 μm × 100 μm) was measured for each analytical point. The analytical time for each lung section was 40–80 h according to the size of the sample.

Preparation and Analysis of Ti Reference Samples

Ti solutions at concentrations of 0.008, 0.02, 0.04, 0.1, 0.2, 0.4, 1 and 2 mg ml^{-1} were prepared by diluting the Ti standard solution (10 mg ml^{-1} of Ti in water with trace HF; Wako Pure Chemical Industries, Ltd., Osaka, Japan) with the tartrazine solution (0.1% in ultrapure water) for coloring the Ti solutions. Then, 0.8 μl of the tartrazine solution (blank) and Ti solutions were dropped on the glass slide (MAS-coated glass slide; Matsunami Glass Ind., Ltd., Osaka, Japan) or on untreated rat lung sections (thickness: 3 μm, with no hematoxylin and eosin stain) mounted onto glass slides with a micropipette. The colored droplets were spread and instantly dried up. Then, the intensities of Ti in these reference samples (representative images as shown in Fig. 3) were analyzed using XRF microscopy (step size: 100 μm).

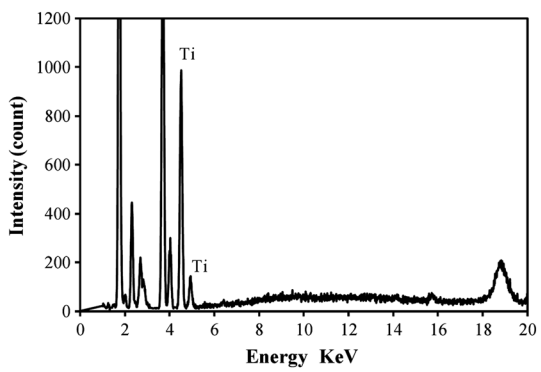

Figure 2. The representative spectra of Ti in the Ti reference samples (2 mg ml^{-1}), which were prepared by dropping different concentrations of Ti solutions (0.8 μl) on the surface of untreated rat lung sections mounted onto the glass slides. The spectral intensity of the Ti-K_α line (Ti-K_α: 4.511 keV; Ti-K_β: 4.932 keV) was acquired for the quantification of Ti.

Tartrazine was used for coloring the Ti droplets because it allowed us to confirm clearly the range of Ti droplets dried on the surfaces of the glass slide and lung sections with the charge-coupled device camera of XRF microscopy. In this work, eosin Y ($C_{20}H_8Br_4O_5$, an acidic pigment, 1% solution) and three acid-fast pigments, including tartrazine ($C_{16}H_9N_4Na_3O_9S_2$), allura red ($C_{18}H_{14}N_2Na_2O_8S_2$) and acid red 52 ($C_{27}H_{29}N_2NaO_7S_2$) (Wako Pure Chemical Industries, Ltd.), were used to screen suitable pigments for coloring the Ti droplets. As shown in Table 1, tartrazine was more suitable for coloring the droplets of Ti because the dried tartrazine droplets had the following features: (i) they allowed for sharply defined images under the charge-coupled device camera; (ii) the nonreduced size more than the wet droplet eliminated the possibility of Ti existence beyond the range of the dried droplet; and (iii) Ti was not detected using XRF analysis.

The calibration curves, which represented the relationship between the Ti content (*x*-axis) and the Ti net intensities (*y*-axis) of the reference samples, were created. The net intensity of Ti for each reference sample was calculated by the following equation:

$$I_{net\ of\ Ti\ reference\ sample}\ (\mathrm{cps}) = \sum_{n=1}^{N} (I_n - I_b) \qquad (1)$$

where $I_{\text{net of Ti reference sample}}$ is the net intensity of Ti for each Ti reference sample; N is the number of analytical points for each Ti reference sample; I_n is the intensity (cps) of Ti for each analytical point; and I_b is the average intensity (cps) of Ti for the blank (the dried tartrazine droplet). Approximately 250 points and 500 points were analyzed for the reference samples on the lung sections and glass slide, respectively.

Derivation of the Detection Limit of TiO_2

Data describing the TiO_2 NP content for each lung section from untreated rat were calculated from the intensities of Ti measured with XRF microscopy (step size: 200 μm) in the corresponding section. Based on the maximum value of the standard deviation (SD_{max}) of the data obtained in lung sections, the detection limit (DL) of TiO_2 was defined as three times the SD_{max}.

Evaluation of Reproducibility

To validate the reproducibility for short-duration analysis of Ti intensity, five repeated measurements were performed using lung sections of the right cranial lobes from untreated rat and TiO_2-treated rat (10 mg kg^{-1} BW) under the same analysis conditions as described above.

As it was necessary to spend a long time on the analysis of the series, the reproducibility of the Ti intensity data was checked once every 2 months for 6 months using the Ti reference samples (0.04 mg Ti ml^{-1} and Ti blank). Furthermore, the effects of

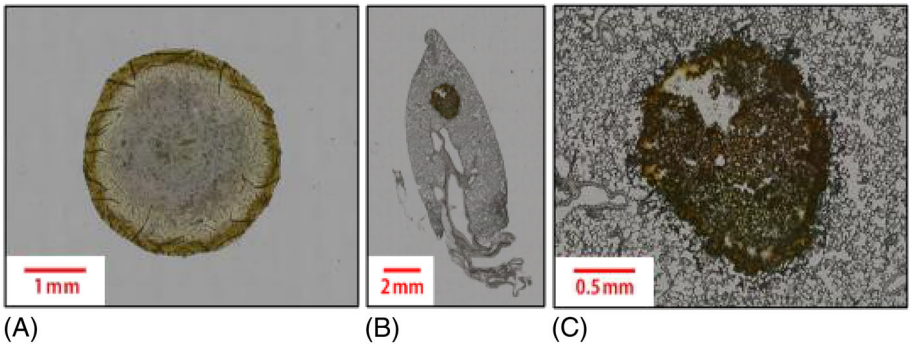

Figure 3. Representative images of the Ti reference samples, which were dried droplets of Ti solutions at different concentrations on the surface of the glass slide (A) and the untreated rat lung sections mounted onto the glass slide (B,C); (C) a magnified image of the spot in (B).

Table 1. Selection of the pigments for coloring the droplets of Ti

Pigment	No precipitate	Sharply defined image	Non-reduced size	No detection of Ti
Eosin	×	–	–	–
Allura Red	○	△	○	–
Acid Red 52	○	△	△	–
Tartrazine	○	○	○	○

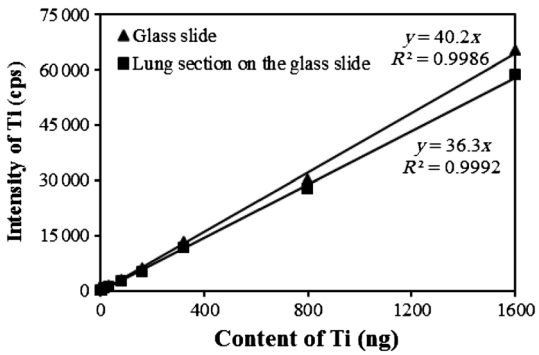

Figure 4. The calibration curves obtained from the different concentrations of Ti droplets (0.8 μl) dried on the glass slide (▲) or on the untreated rat lung sections (thickness: 3 μm) mounted onto the glass slides (■).

the X-ray tube replacement on the Ti intensity were also investigated by evaluating variations in the net intensity of the Ti reference sample (0.04 mg Ti ml^{-1}) after the X-ray tube was replaced.

Quantification of the Pulmonary Microdistribution of TiO_2

Lung sections (thickness: 3 μm) prepared from the left and right lung lobes of TiO_2-treated rats were used to analyze Ti intensities with XRF microscopy (step size: 200 μm). The net intensity of each analysis point was calculated by the following equation:

$$I_{net\ of\ each\ analytical\ point}\ (\mathrm{cps}) = I_n\text{-}I_{bg} \quad (2)$$

where $I_{net\ of\ each\ analytical\ point}$ is the Ti net intensity of each analytical point; I_n is the Ti measured intensity of each analytical point; and I_{bg} is the average Ti intensity of the background (i.e. the area of the glass slide that was adjacent to the corresponding lung section) because similar Ti intensities were observed in lung sections from untreated rat and the glass slide. The TiO_2 content in the mesh (100 μm × 100 μm) was quantified based on the Ti calibration curve obtained from the Ti reference samples on lung sections from untreated rat in the present study.

Results

Calibration Curves of Ti

The calibration curves of Ti are shown in Fig. 4. The linear relationships between the intensities of Ti and the content of Ti were observed in both Ti reference samples on the glass slide (slope: 40.2, $R^2 = 0.9986$) and on the lung sections mounted onto the glass slides (slope: 36.3, $R^2 = 0.9992$).

The sizes of Ti reference samples on the glass slide were significantly larger (by about twofold) than those on the lung sections. With respect to the Ti reference samples on the lung sections, the values of Ti average content were (in ng $mesh^{-1}$): 0.035 (maximum: 0.11), 0.077 (maximum: 0.40), 0.13 (maximum: 0.74), 0.29 (maximum: 1.2), 0.67 (maximum: 2.2), 1.5 (maximum: 6.9), 2.8 (maximum: 21) and 6.1 (maximum: 33) for the reference samples prepared by dropping Ti solutions at concentrations of 0.008, 0.02, 0.04, 0.1, 0.2, 0.4, 1 and 2 mg ml^{-1}, respectively. In contrast, the values of Ti average content were (in ng $mesh^{-1}$): 0.0083 (maximum: 0.12), 0.028 (maximum: 0.41), 0.066 (maximum: 0.35), 0.13 (maximum: 0.43), 0.31 (maximum: 0.73), 0.62 (maximum: 1.5), 1.6 (maximum: 4.6) and 3.2 (maximum: 5.3) for the Ti reference samples on the glass slide prepared by 0.008, 0.02, 0.04, 0.1, 0.2, 0.4, 1 and 2 mg ml^{-1} Ti solution, respectively. These observations showed the uneven distribution of Ti in the reference samples developed in this study and suggested that the ranges of Ti quantification were 0.059–6.1 ng $mesh^{-1}$ and 0.0083–3.2 ng $mesh^{-1}$ for the calibration curves obtained from the reference samples on lung sections of untreated rat and on the glass slide, respectively.

Detection Limit of TiO_2 Nanoparticles

The SDs of TiO_2 content in the mesh (100 μm × 100 μm) were 0.021 ng $mesh^{-1}$ for lung sections of the left and right cranial and caudal lobes and 0.020 ng $mesh^{-1}$ for those of the right middle and accessory lobes from the untreated rat. These values

were similar to those obtained from the background (glass slides, 0.020–0.023 ng mesh^{-1}). Based on the three times SD_{max} value (i.e. 0.021 ng mesh^{-1}) obtained from lung sections of untreated rat, the DL of TiO_2 was estimated to be 0.063 ng mesh^{-1} (6.3 ng mm^{-2}).

Data Reproducibility

Data variations for short-duration measurements are shown in Fig. 5. During five repeated measurements, the relative SDs (RSDs) of the average intensities were 0.91% for the whole lung

A

	Lung section of untreated rat		Lung section of TiO_2-treated rat (10 mg kg^{-1} BW)	
	Glass slide	Lung area	Glass slide	Lung area
Average intensity of Ti (cps, ± SD)	1.03 ± 0.006	1.03 ± 0.016	1.02 ± 0.018	2.84 ± 0.026
RSD (%)	0.57	1.5	1.7	0.91

B

	Lung section of untreated rat		Lung section of TiO_2-treated rat (10 mg kg^{-1} BW)					
	Glass slide	Lung area	Glass slide	Lung area				
Content of TiO_2 (ng mesh^{-1})	—DL	—DL	—DL	—DL	DL—0.3	0.3—0.6	0.6—0.9	0.9—
Intensity of Ti (cps)	—2.32	—2.32	—2.31	—2.31	2.31—7.45	7.45—13.9	13.9—20.3	20.3—
Average RSD (%)	40.5	40.2	40.5	38.9	21.1	12.5	10.7	8.59
Range of RSD (%)	5.49—135	7.70—125	4.86—98.9	5.28—107	2.76—60.2	2.67—33.5	1.19—23.5	1.76—22.6

C

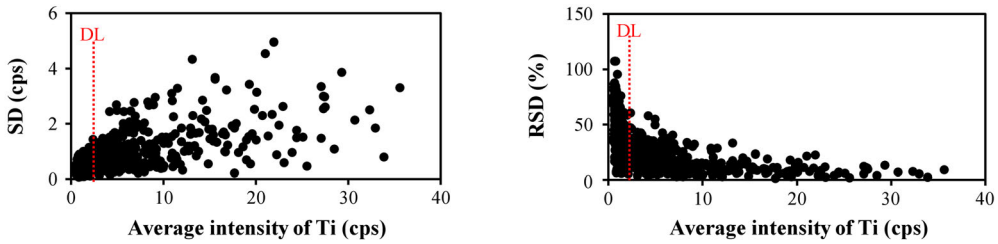

Figure 5. Variations in data during five repeated measurements of Ti intensities in lung sections (right cranial) from untreated rat and TiO_2-treated rat (10 mg kg^{-1} BW). (A) Variations in the total average values of Ti in lung areas and the adjacent background (glass slide). (B) Variations in Ti average intensities for the analysis points of each intensity (content) range in lung areas and adjacent background. (C) Variations in Ti average intensities for each analysis point in lung area of the right cranial lobe from TiO_2-treated rat. BW, body weight; DL, detection limit of TiO_2 NPs (0.063 ng mesh^{-1}); RSD, relative SD.

Table 2. Pulmonary microdistribution (100 μm × 100 μm) of TiO_2 nanoparticles (AEROSIL® P25) in the sections of right and left lung lobes from rats ($n = 3$) treated with 10 mg kg^{-1} BW TiO_2 nanoparticles

Lung section	Rat no.	Content of TiO_2 (ng mesh^{-1})		95%ile content of TiO_2 (ng mesh^{-1})	Detection rate of TiO_2 (%)
		Average	Min–max		
Right cranial	1	0.066	ND–1.3	0.38	25.0
	2	0.039	ND–1.0	0.28	16.6
	3	0.069	ND–1.8	0.52	19.3
Right middle	1	0.028	ND–0.73	0.21	13.0
	2	0.0084	ND–0.78	0.065	5.19
	3	0.041	ND–1.2	0.27	15.6
Right caudal	1	0.17	ND–2.1	0.86	39.2
	2	0.12	ND–3.6	0.67	28.6
	3	0.10	ND–1.8	0.54	33.7
Right accessory	1	0.20	ND–2.8	0.97	38.7
	2	0.12	ND–1.9	0.61	37.1
	3	0.059	ND–1.3	0.39	21.4
Left	1	0.016	ND–0.50	0.13	10.6
	2	0.050	ND–1.2	0.30	23.2
	3	0.041	ND–0.93	0.27	18.6

DL, detection limit; ND, not detectable.
Data indicated as ND were calculated as 0 ng mesh^{-1}. The DL of TiO_2 NPs was 0.063 ng mesh^{-1} (per 100 μm × 100 μm mesh). The detection rate of TiO_2 was the percentage of the detected analytical points to all analytical points of Ti in each lung section.

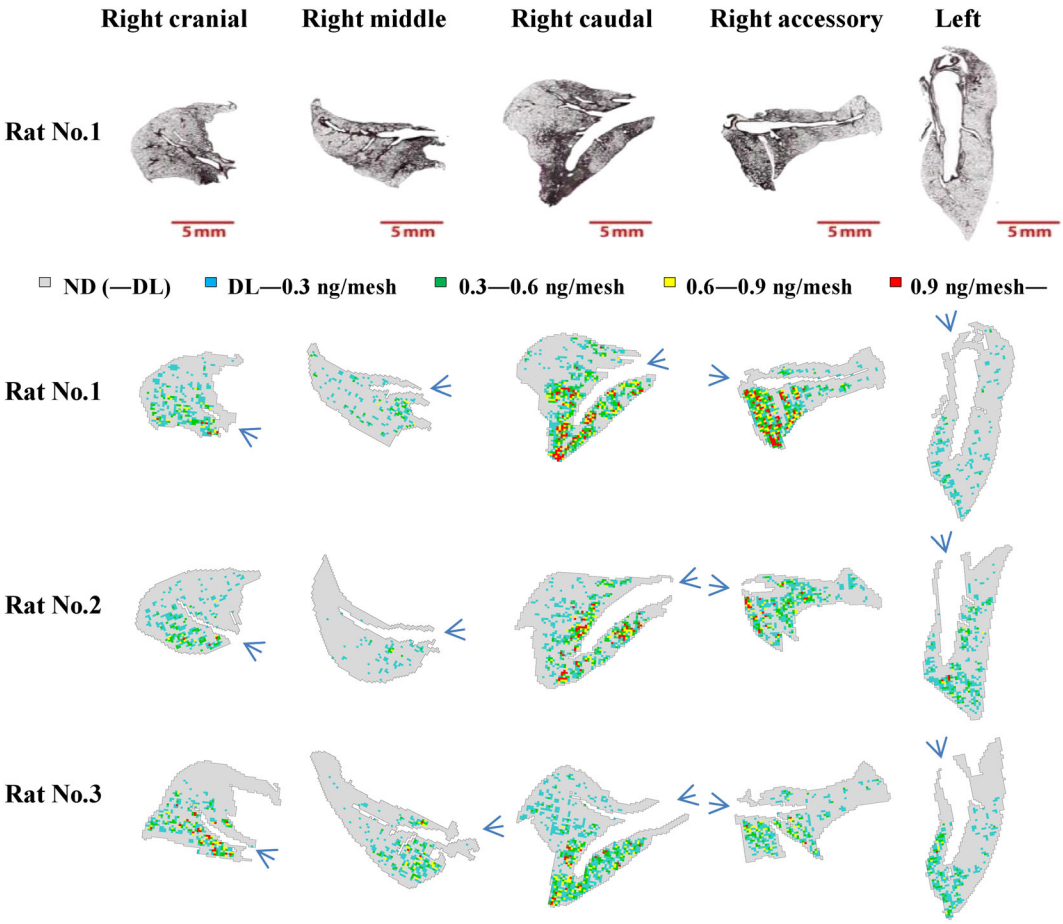

Figure 6. Representative optical images (top line) and quantitative maps of the pulmonary microdistribution of TiO_2 (from the second line to the fourth line) in lung sections of right and left lobes from rats treated with 10 mg kg^{-1} BW TiO_2 NPs. The Ti intensities in lung sections were acquired using X-ray fluorescence microscopy (XGT-7200). The detection limit of TiO_2 was 0.063 ng $mesh^{-1}$. The suspension of TiO_2 NPs entered the lung through the lung hilum (indicated by the direction of the arrows). The direction of lung sections represents the actual direction of lung lobes when the rats were administered TiO_2 NPs. BW, body weight; NPs, nanoparticles.

section of TiO_2-treated rats (10 mg kg^{-1} BW) and 0.57–1.7% for the glass slide and lung sections of untreated rat (Fig. 5A).

As shown in Fig. 5(B,C), the average RSDs of Ti intensities for each analytical point in the right cranial lobe section of lung from TiO_2-treated rat (10 mg kg^{-1} BW) tended to decrease from 38.9% for the range below the DL (maximum: 107%) to 8.59% for the range above 0.9 ng $mesh^{-1}$ (maximum: 22.6%) with the increase in Ti intensity (i.e. the content of TiO_2 NPs, ng $mesh^{-1}$). The average RSD was 21.1% (maximum: 60.2%) for each analytical point in the range of DL-0.3 ng $mesh^{-1}$.

With regard to data variations for long-duration measurements, the net intensities of the Ti reference sample (0.04 mg Ti ml^{-1}) increased by 3.4%, 0.81% and 2.2% after 2, 4 and 6 months, respectively. In contrast, the net intensity of the 0.04 mg ml^{-1} Ti standard increased by 28% after the X-ray tube was replaced.

Quantitative Evaluation of the Pulmonary Microdistribution of TiO_2 Nanoparticles

Data on the pulmonary quantitative microdistribution (per mesh: 100 μm × 100 μm, step size: 200 μm) of TiO_2 NPs in lung sections of the right and left lobes from TiO_2-treated rats (10 mg kg^{-1} BW, $n = 3$) are shown in Table 2 and Fig. 6. The directions of lung sections shown in Fig. 6 represent the actual directions of lung lobes when the rats were intratracheally administered the suspension of TiO_2 NPs.

Data on the pulmonary microdistribution of TiO_2 NPs indicated that TiO_2 NPs were unevenly distributed in the lung. Although we were not certain that the lung sections provided sufficient representation of the overall distributions of TiO_2, our results suggested that the right caudal (0.13 ± 0.036 ng $mesh^{-1}$) and accessory (0.13 ± 0.071 ng $mesh^{-1}$) lobes deposited more TiO_2 NPs followed by the right cranial (0.058 ± 0.017 ng $mesh^{-1}$), left (0.036 ± 0.018 ng $mesh^{-1}$) and right middle (0.026 ± 0.016 ng $mesh^{-1}$) lobes (Table 2).

By quantitatively evaluating the pulmonary microdistribution of TiO_2 NPs using lung sections from TiO_2-treated rats, we found that the detection rates (the percentage of the detected analytical points for all analytical points of Ti in each lung section) of TiO_2 NPs were 33.8 ± 5.30% for the right caudal, 32.4 ± 9.56% for the right accessory, 20.3 ± 4.29% for the right cranial, 17.5 ± 6.38% for the left and 11.3 ± 5.42% for the right middle lobe sections (Table 2).

Discussion

In the present study, we established a quantitative method for evaluating the pulmonary microdistribution of TiO_2 NPs in rats

using XRF microscopy. We prepared Ti reference samples by dropping different concentrations of Ti solutions on glass slides and on lung sections from untreated rat. The good linearity of the Ti intensity with the Ti content confirmed the validity of the calibration. The similarities of the slopes for the calibration curves on both substrates suggested that the matrix effect was small in the ultrathin lung sections for the quantification of Ti.

The preparation of reference samples with an even distribution of metal elements was complicated (Homma-Takeda *et al*., 2009; Rubio *et al*., 2008; Watanabe *et al*., 2001). In this study, the reference samples were simply prepared, and a good linear correlation of the Ti intensity with the Ti content was observed, despite the somewhat uneven distribution of Ti in the reference samples.

With respect to data reproducibility using the developed Ti calibration curve, we performed a short-term study of five repeated measurements and a long-term study (6 months) of measurements. For five repeated measurements, the RSDs of the average intensities were 0.91% for the whole lung sections of TiO_2-treated rats (10 mg kg^{-1} BW) and from 0.57% to 1.7% for the glass slide and lung sections of untreated rat (Fig. 5A). Geraki *et al*. (2002) reported that the RSDs for Fe, Cu and Zn were 19%, 40% and 21% when the diseased breast tissue specimen was measured 10 times using synchrotron radiation-induced XRF. These results indicated that there were relatively small changes in the average intensities of Ti in lung sections for short-duration measurements in the current study. For the variations in Ti intensities of each analytical point, the average RSDs were 21.1% (maximum: 60.2%), 12.5% (maximum: 33.5%), 10.7% (maximum: 23.5%) and 8.59% (maximum: 22.6%) for the ranges of DL-0.3 ng $mesh^{-1}$, 0.3–0.6 ng $mesh^{-1}$, 0.6–0.9 ng $mesh^{-1}$ and above 0.9 ng $mesh^{-1}$, respectively. This variation would not be expected to affect the pulmonary microdistribution of TiO_2 NPs because the data variations for each analytical point were much smaller than the distribution range of the detected TiO_2 NPs (0.063–1.8 ng $mesh^{-1}$ in whole lung sections from the right cranial lobe of rat no. 3, Table 2, which indicated a difference of about 30-fold in the distribution range).

The calibration curve should be recalibrated after replacement of the X-ray tube to ensure high data reproducibility, as the net intensity of the Ti standard increased by 28% after the X-ray tube was replaced. Correction of the calibration curve should be performed at least once every 2 months to ensure data reliability, although the variations during the current long-term study were confirmed to be quite small.

The distribution of TiO_2 NPs measured in the present study could represent the administered TiO_2 NPs as TiO_2 NPs are insoluble particles and the Ti background was very small. In our examination of the appropriateness of the Ti calibration curve for TiO_2 quantification in lung sections from TiO_2-treated rats, the data for detected TiO_2 NP content ranged from DL (0.063 ng TiO_2 $mesh^{-1}$, i.e. 0.038 ng Ti $mesh^{-1}$) to 3.6 ng $mesh^{-1}$ (i.e. 2.2 ng Ti $mesh^{-1}$), as shown Table 2; these values were in the range of Ti quantification (0.035–6.1 ng Ti $mesh^{-1}$) in the calibration curve obtained from the reference samples on lung sections from untreated rats. This observation implied the accuracy of the quantitative values of TiO_2 content in a mesh in the current study.

With regard to the pulmonary TiO_2 NPs microdistribution in the TiO_2-treated rats (10 mg kg^{-1} BW), the right middle lobes received relatively less TiO_2 NPs compared with the other lobes, which was similar to the results of previous studies (Brain *et al*., 1976; Leong *et al*., 1998), in which the lung lobes of rats intratracheally administered with particles (^{99m}Tc, dye) were cut into several pieces to confirm the distribution patterns of the administered particles. However, we did not observe a high content of TiO_2 NPs in the left lobes, inconsistent with the results described by Brain *et al*. (1976) and Leong *et al*. (1998), who observed the deposition of more particles (^{99m}Tc, dye) in the left lobes of rats. This apparent discrepancy may be due to the differences in administration techniques (e.g. difference in the administration tools used in the two studies and the insertion position of the needle for the administration) and/or the time points at which the pulmonary distribution was observed.

From the quantitative results regarding the TiO_2 microdistribution, TiO_2 NPs appeared to be easily deposited in lung lobes located downstream of the administration direction of the NP suspension, e.g. the right caudal and accessory lobes (Fig. 6, the directions of lung sections represent the actual directions of lung lobes when the rats were intratracheally administered the suspension of TiO_2 NPs). The data also suggested that more TiO_2 NPs were distributed in the tissues adjacent to the airway, and the lower portion of each lung lobe (Fig. 6). This was supported by a study by Brain *et al*. (1976), in which intratracheal administration with labeled particles (^{99m}Tc) resulted in less deposition in apical areas and greater amounts in basal regions of every lobe.

In addition, some toxicological studies of NPs following intratracheal administration have used sections from a specific lobe of the lung, e.g. the left lobe, for histopathological examination (Han *et al*., 2011; Ogami *et al*., 2009). Our results indicated that there were large variations in the pulmonary microdistribution of administered NPs among the lobes of the lung, suggesting that histopathological examinations should be performed for all sections of all lobes of the lung to avoid the over- and underestimation of pathological responses caused by NP administration.

In summary, we quantitatively evaluated the pulmonary microdistribution of TiO_2 NPs in rats following intratracheal administration with 10 mg kg^{-1} BW TiO_2 NPs. To this end, we developed a new method for quantifying the microdistribution of Ti, which had the following features: (i) the preparation method for the Ti reference samples was simple, and a good linear relationship was found between the Ti intensity and Ti content; (ii) the correction for matrix effects was unnecessary because the Ti reference samples and the analytical samples (lung sections) had the same matrix and thickness; and (iii) there was sufficient data reproducibility. These data describing the pulmonary quantitative microdistribution of NPs are important for comparing differences in NP distributions following intratracheal administration and inhalation exposure and for assessing the standardization of test methods for intratracheal administration. Quantification of the pulmonary microdistribution of NPs would be useful for establishing a relationship between the content of localized NPs and the pathological responses in a localized region of the lung. Moreover, this method may also be applied for evaluating the clearance of pulmonary NPs in microscopic areas, e.g. the pattern of clearance. Further studies are needed to examine these processes. We believe that analysis of the quantitative microdistribution of NPs will contribute to our toxicological understanding of NPs. This method can also be applied to other metal/metal oxide NPs in biological samples.

Acknowledgments

The authors wish to thank Miss Tomoko Yanagibashi and Mr. Yoshihiro Gamo, National Institute of Advanced Industrial Science and Technology, for their valuable contributions to create the figures in this paper. This work was part of the research program entitled "Development of innovative methodology for safety assessment of industrial nanomaterials," supported by the Ministry of Economy, Trade, and Industry (METI) of Japan.

References

Auriat AM, Silasi G, Wei ZP, Paquette R, Paterson P, Nichol H, Colbourne F. 2012. Ferric iron chelation lowers brain iron levels after intracerebral hemorrhage in rats but does not improve outcome. *Exp. Neurol.* **234**:136–143.

Brain JD, Knudson DE, Sorokin SP, Davis MA. 1976. Pulmonary distribution of particles given by intratracheal instillation or by aerosol inhalation. *Environ. Res.* **11**:13–33.

Driscoll KE, Costa DL, Hatch G, Henderson R, Oberdorster G, Salem H, Schlesinger RB. 2000. Intratracheal instillation as an exposure technique for the evaluation of respiratory tract toxicity: uses and limitations. *Toxicol. Sci.* **55**:24–35.

Geraki K, Farquharson MJ, Bradley DA. 2002. Concentrations of Fe, Cu and Zn in breast tissue: a synchrotron XRF study. *Phys. Med. Biol.* **47**:2327–2339.

Han B, Guo J, Abrahaley T, Qin LJ, Wang L, Zheng YD, Li B, Liu DD, Yao HC, Yang JW, Li CM, Xi ZG, Yang X. 2011. Adverse effect of nano-silicon dioxide on lung function of rats with or without ovalbumin immunization. *PLoS One* **6**(2):e17236(1–8).

Homma-Takeda S, Terada Y, Nakata A, Sahoo SK, Yoshida S, Ueno S, Inoue M, Iso H, Ishikawa T, Konishi T, Imaseki H, Shimada Y. 2009. Elemental imaging of kidneys of adult rats exposed to uranium acetate. *Nucl. Instrum. Methods Phys. Res. B.* **267**:2167–2170.

Jacobsen NR, Moller P, Jensen KA, Vogel U, Ladefoged O, Loft S, Wallin H. 2009. Lung inflammation and genotoxicity following pulmonary exposure to nanoparticles in ApoE(-/-) mice. *Part. Fibre Toxicol.* **6**:2(1–17).

Khodadoust S, Sheini A, Armand N. 2012. Photocatalytic degradation of monoethanolamine in wastewater using nanosized TiO_2 loaded on clinoptilolite. *Spectrochim. Acta. A* **92**:91–95.

Leong BKJ, Coombs JK, Sabaitis CP, Rop DA, Aaron CS. 1998. Quantitative morphometric analysis of pulmonary deposition of aerosol particles inhaled via intratracheal nebulization, intratracheal instillation or nose-only inhalation in rats. *J. Appl. Toxicol.* **18**:149–160.

NRC. 1996. *Guide for the Care and Use of Laboratory Animals*. National Research Council, National Academy Press: Washington, DC.

Ogami A, Morimoto Y, Myojo T, Oyabu T, Murakami M, Todoroki M, Nishi K, Kadoya C, Yamamoto M, Tanaka I. 2009. Pathological features of different sizes of nickel oxide following intratracheal instillation in rats. *Inhal. Toxicol.* **21**(8–11):812–818.

Reuzel PG, Bruijntjes JP, Feron VJ, Woutersen RA. 1991. Subchronic inhalation toxicity of amorphous silicas and quartz dust in rats. *Food Chem. Toxicol.* **29**(5):341–354.

Rubio M, Perez RD, Perez CA, Eynard AH, Bongiovanni GA. 2008. Synchrotron microscopic X-ray fluorescence analysis of the effects of chronic arsenic exposure in rat brain. *Radiat. Phys. Chem.* **77**:1–8.

Shi HB, Magaye R, Castranova V, Zhao JS. 2013. Titanium dioxide nanoparticles: a review of current toxicological data. *Part. Fibre Toxicol.* **10**:15(1–33).

Shinohara N, Oshima Y, Kobayashi T, Imatanaka N, Nakai M, Ichinose T, Sasaki T, Zhang G, Fukui H, Gamo M. 2014. Dose-dependent clearance kinetics of intratracheally administered titanium dioxide nanoparticles in rat lung. *Toxicology* **325**:1–11.

Su CY, Tang HZ, Zhu GD, Li CC, Lin CK. 2014. The optical properties and sunscreen application of spherical h-BN-TiO_2/mica composite powder. *Ceram. Int.* **40**:4691–4696.

Sun QQ, Tan DN, Ze YG, Sang XZ, Liu XR, Gui SX, Cheng Z, Cheng J, Hu RP, Gao GD, Liu G, Zhu M, Zhao XY, Sheng L, Wang L, Tang M, Hong FS. 2012. Pulmotoxicological effects caused by long-term titanium dioxide nanoparticles exposure in mice. *J. Hazard. Mater.* **235-236**:47–53.

Sung JH, Ji JH, Park JD, Yoon JU, Kim DS, Jeon KS, Song MY, Jeong J, Han BS, Han JH, Chung YH, Chang HK, Lee JH, Cho MH, Kelman BJ, Yu IJ. 2009. Subchronic inhalation toxicity of silver nanoparticles. *Toxicol. Sci.* **108**(2):452–461.

Wang JX, Chen CY, Yu HW, Sun J, Li B, Li YF, Gao YX, He W, Huang YY, Chai ZF, Zhao YL, Deng XY, Sun HF. 2007. Distribution of TiO_2 particles in the olfactory bulb of mice after nasal inhalation using microbeam SRXRF mapping techniques. *J. Radioanal. Nucl. Ch.* **272**:527–531.

Wang JX, Chen CY, Liu Y, Jiao F, Li W, Lao F, Li YF, Li B, Ge CC, Zhou GQ, Gao YX, Zhao YL, Chai ZF. 2008. Potential neurological lesion after nasal instillation of TiO_2 nanoparticles in the anatase and rutile crystal phases. *Toxicol. Lett.* **183**:72–80.

Wang HJ, Wang M, Wang B, Meng XY, Wang Y, Li M, Feng WY, Zhao YL, Chai ZF. 2010. Quantitative imaging of element spatial distribution in the brain section of a mouse model of Alzheimer's disease using synchrotron radiation X-ray fluorescence analysis. *J. Anal. Atomic Spectrom.* **25**:328–333.

Watanabe K, Miyakama O, Kobayashi M. 2001. New method for quantitative mapping of metallic elements in tissue sections by electron probe microanalyser with wavelength dispersive spectrometers. *J. Electron Microsc.* **50**:77–82.

Yin ZF, Wu L, Yang HG, Su YH. 2013. Recent progress in biomedical applications of titanium dioxide. *Phys. Chem. Chem. Phys.* **15**:4844–4858.

Zhu MT, Feng WY, Wang Y, Wang B, Wang M, Ouyang H, Zhao YL, Chai ZF. 2009. Particokinetics and extrapulmonary translocation of intratracheally instilled ferric oxide nanoparticles in rats and the potential health risk assessment. *Toxicol. Sci.* **107**(2):342–351.